

**INVESTIGATION OF THE STRUCTURE OF THE  
ELECTROMAGNETIC FIELD AND RELATED PHENOMENA,  
GENERATED BY THE "ACTIVE" SATELLITE**

**Grant NAG5-1340**

**FINAL REPORT**

**For the period May 1, 1990 through April 30, 1992**

**Principal Investigator**

**Dr. Yakov L. Alpert**

**June 1992**

**Prepared for  
National Aeronautics and Space Administration  
Greenbelt, Maryland 20771**

**Smithsonian Institution  
Astrophysical Observatory  
Cambridge, Massachusetts 02138**

**The Smithsonian Astrophysical Observatory  
is a member of the  
Harvard-Smithsonian Center for Astrophysics**

**The NASA Technical Officer for this grant is Mr. Paul Pashby, Code 602  
Goddard Space Flight Center, Greenbelt, Maryland 20771**

**(NASA-CR-190446) INVESTIGATION OF THE  
STRUCTURE OF THE ELECTROMAGNETIC FIELD AND  
RELATED PHENOMENA, GENERATED BY THE ACTIVE  
SATELLITE Final Report, 1 May 1990 - 30 Apr.  
1992 (Smithsonian Astrophysical**

**N92-29568**

**Unclas  
G3/32 0104040**

## **Contents**

### **Abstract**

### **Section I. Introduction**

**Section II.** General properties of the electric field  $|\mathbf{E}|$ , radiated by an electric dipole in a magnetoplasma.

**II.1** Statement of the problem. Equations, formulae.

**II.2** Frequency and angle dependencies of  $|\mathbf{E}|$  in all the regions of their enhancement and focusing.

**Section III.** The electric fields  $|\mathbf{E}|$  at  $\mathbf{Z} = (800 - 6000) \text{ km}$ .

**III.1** Altitude and angle dependencies of  $|\mathbf{E}_0|$  and  $|\mathbf{E}_{\text{res}}|$ .

**III.2** Discussion of the principle properties of  $|\mathbf{E}|$ .

### **Summary**

## Abstract

A short review is given for the general frequency and angle distribution of the electric field radiated by an electric dipole  $\mathbf{E} = \mathbf{E}_0 \cos \omega t$ , in a magnetoplasma. Detailed results of numerical calculations of  $|\mathbf{E}|$  were made in the **VLF** and **LF** frequency bands  $0.02\mathbf{f_b} \leq \mathbf{F} \leq 0.5\mathbf{f_b}$  ( $\mathbf{F} \sim (4-500) \text{ kHz}$ ) in the ionosphere and magnetosphere in the altitude region  $\mathbf{Z} = (800-6000) \text{ km}$ ;  $\mathbf{f_b}$  is the electron gyro-frequency of the plasmas in the discussed region  $\mathbf{f_b} \simeq (1.1 \text{ to } 0.2) \text{ MHz}$ .

The amplitudes of the electric field have large maxima in four regions: close to the direction of the Earth magnetic field line  $|\mathbf{B}_0|$ , it is the so called Axis field  $\mathbf{E}_0$  and in the Storey  $|\mathbf{E}_{St}|$ , Reversed Storey  $|\mathbf{E}_{RevSt}|$ , and Resonance  $|\mathbf{E}_{Res}|$  Cones. The maximal values of  $\mathbf{E}_0$ ,  $\mathbf{E}_{Res}$ , and  $\mathbf{E}_{Rev.St}$  are very pronounced close to the low hybrid frequency,  $\mathbf{F} \sim \mathbf{F_L}$ . The flux of the electric field is concentrated in very narrow regions, the apexes angles of the cones  $\Delta\beta \simeq (0.1 - 1) \text{ degree}$ . The enhancement and focusing of the electric field is growing up, especially quickly at  $\mathbf{Z} > 800 \text{ km}$ . At  $\mathbf{Z} \geq 1000$  up to  $6000 \text{ km}$ , the relative value of  $|\mathbf{E}|$ , in comparison with its value at  $\mathbf{Z} = 800 \text{ km}$  is about  $(10^2 \text{ to } 10^4)$  times larger. Thus, the flux of **VLF** and **LF** electromagnetic waves in the Earth magnetoplasma produces and is guided by very narrow *pencil beams*, similar, let us say, to laser beams.

## I. Introduction

Some results of theoretical calculations provided by the Grant NAG5-1340 (see [1]) of the electric field radiated in the ionosphere by a VLF-LF transmitter, placed on a Satellite, and of the heating of the surrounding magnetoplasma under the action of this generator, were presented in three previous Semi-Annual reports. It was supposed that both of these phenomena will be studied experimentally in situ. Namely by different sets placed on the Satellite and on a Sub-Satellite, moving around the mother Satellite.

In the Semi-Annual report # 2 the study of the non-linear heating was completed. All the results of these calculation are presented there in details. In this report, the completed results of the study of the electric field are presented in detail. They include calculations of the field  $|\mathbf{E}|$  in the ionosphere up to the low region of the magnetosphere ( $Z = 6000 \text{ km}$ ), i.e. along the trajectories of propagation of VLF and LF electromagnetic field lines  $\mathbf{B}_0$  of the Earth. The presented results of these calculations were done by the computer of the Goddard Space Flight Center in collaboration with Dr. James Green.

The results obtained are interesting and, in a sense, unexpected. It will be interesting and important to extend such calculations for large distances from the Earth, for values of  $L = R/R_0 \simeq (2 - 5)$ ;  $R_0$  is the radius of the Earth.

## II. General properties of the electric field $|E|$ .

The linear theory of radiation of an electric dipole in a magnetoplasma, used in this study, was developed by Alpert, Alpert & Moiseyev ([2] and [3]), and by Alpert, Budden, et al. (see [4], [5]). The general theoretical results obtained in these papers, namely the main formulae, the computer program and the general physical understanding of this problem, are used in this study. Some results of these calculations are presented in this section for producing a general picture of the structure of the electromagnetic field radiated by a *mother satellite* moving in the ionosphere in neighborhood of this satellite. Besides, it is supposed that this field is recorded on the far zone of this source by a *child sub-satellite*, moving around the mother satellite at distances from it  $r$  about 100 and more kilometers. Then the theory for a homogeneous medium may be used at the altitudes of the ionosphere discussed here and in the magnetosphere for calculations of the electric field around the mother body. It is a sufficiently good approximation because at the altitudes interesting for us on such distances  $r$  from the mother body, the magnetosphere may be considered as a homogeneous medium. It is also supposed that the local parameters of the magnetoplasma in the neighborhood of these bodies (the electron and ion densities, the collision frequencies, the magnetic field, etc.) are estimated by this experiment simultaneously with the recording of the amplitudes of the electric field.

## II.1 Statement of problem, formulae.

An homogeneous cold magnetoplasma, which is characterized by a superimposed magnetic field  $\mathbf{B}_0$ , by an electric permittivity tensor  $\epsilon_0$  and a refractive index  $\mathbf{n}$  is considered. The magnetic field  $\mathbf{B}_0$  is parallel to the  $\mathbf{z}$  axis in the cartesian  $(x, y, z)$  and in the cylindrical  $(\rho, \varphi, z)$  coordinate systems. The refractive index is thought as a vector  $\mathbf{n}$  with components

$$\begin{aligned} n_x &= n \sin \Theta \cos \varphi, \quad n_y = n \sin \Theta \cdot \sin \varphi, \quad n_z = n \cos \Theta, \\ n_\varphi^2 &= (n_x^2 + n_y^2) = n^2 \sin^2 \Theta, \end{aligned} \quad (1)$$

where  $\Theta$  is the angle between the wave normal vector  $\mathbf{k}$  and the  $\mathbf{z}$  axis,  $\mathbf{z} \parallel \mathbf{B}_0$ . The electromagnetic waves  $\mathbf{E}, \mathbf{H} \sim e^{i\omega t}$ , generated in the magnetoplasma, are produced by an electric dipole of moment  $\mathbf{I}e^{i\omega t}$ ,  $\omega = 2\pi F$  or  $\omega = 2\pi f$  is the angular frequency of the waves. The electric dipole is parallel to the  $\mathbf{z}$  axis, i.e.  $\mathbf{I} \parallel \mathbf{B}_0$ . The source dipole is placed at  $x = y = z = 0$ , i.e. on the mother satellite. The receiving point is at a distance  $r = \sqrt{x^2 + z^2}$  from the source in a direction  $\beta$  to the magnetic field  $\mathbf{B}_0$  and

$$x = r \sin \beta, \quad y = 0, \quad z = r \cos \beta \quad (2)$$

since the plasma has rotational symmetry around the  $\mathbf{z}$  axis.

The general solution of the system of the Maxwell equations of this problem is described by a sum of complicated integrals (see [3], [4]). The integrands of these integrals are rapidly oscillating functions. They are described by the Bessel functions  $J_0(n_\perp, \frac{\omega}{c}\rho)$  and  $J_1(n_\perp, \frac{\omega}{c}\rho)$ , and the derivatives  $\frac{dn_\parallel}{dn_\perp}$

where

$$n_{\perp} = n \sin \Theta, \quad n_{\parallel} = n \cos \Theta, \quad n^2 = n_{\perp}^2 + n_{\parallel}^2.$$

These integrals may be studied only by numerical methods. The method of the steepest descents, i.e. the stationary phase method, was used for this purpose. Certainly, the accuracy of this asymptotic method is sufficiently high only in the far zone from the source, namely, when

$$\frac{\omega}{c} \sqrt{\rho^2 + z^2} = \frac{\omega}{c} r \gg 1. \quad (3)$$

The *main contribution* to the field is made by saddle points. Two cases should be considered by analyzing the integrals. Namely these cases characterize the basic physical properties of the field.

The first case is when the observation point - the receiver - is at very small horizontal distances from the source, namely, when  $x \sim 0$ , i.e. the angle  $\beta$  of the ray direction is very small. In this region the field is growing up and *becomes very strong* close to the direction of the magnetic field. It is called the *Axis field*  $\mathbf{E}_0$ . The saddle points are estimated in this case by the equation

$$\frac{dn_{\parallel}}{dn_{\perp}} = 0 \quad (4)$$

The Axis field *enhancement* appears at frequencies  $\omega \geq \omega_L$ ,  $\omega_L = 2\pi F_L$  is the low hybrid frequency. This is one of the most interesting peculiarities of this problem. For many decades, an erroneous conclusion was in the literature that the field disappears close to the direction of the magnetic field  $\mathbf{B}_0$  (see, for example, Arbel and Felson [6]).

The second important case is when  $n_{\perp}\rho \gg 1$  and the observation point is sufficiently far from the axis, from the direction of the magnetic field  $\mathbf{B}_0$ , and the asymptotic of the Bessel function

$$J_0, J_1 \sim (2\pi n_{\perp}\rho)^{1/2} \exp \left[ -i \left( n_{\perp}\rho - \frac{\pi}{4} \right) \right] \quad (5)$$

may be used. The saddle points are estimated in this region by the equation

$$\cos \beta \frac{dn_{\parallel}}{dn_{\perp}} + \sin \beta = 0 \quad (6)$$

The field is enhanced in that region again because of the contributing of two saddle points of the integrands when they are close together - they coalesce. The field is enhanced in this case in different angle intervals  $\beta$ . They are  $\mathbf{E}_{St}$  and  $\mathbf{E}_{Rev.St}$  and form Storey and Reversed Storey cones called by us. They respectively exist in the frequency bands  $F_{RS} \leq F \leq F_{S2}$  and  $F_{RS} \leq F \leq F_L$  (see below Fig.1). The field  $E_{Rev.St}$  becomes especially strong at frequencies  $\omega \leq \omega_L$ .

One more region of the enhancement of the field  $E_{Res}$  is the *resonance cone*. It occurs when the coefficient of refraction  $n \rightarrow 0$ . At the resonance

$$\Theta - \beta = \pm \frac{\pi}{2}, \quad \tan^2 \beta = -\frac{\varepsilon_{xx}}{\varepsilon_{zz}}, \quad (7)$$

where  $\varepsilon_{xx}$  and  $\varepsilon_{zz}$  are the elements of the tensor  $\varepsilon_0$ . In our case, in the cartesian coordinate system

$$\varepsilon_0 = \begin{bmatrix} \varepsilon_{xx} & \varepsilon_{xy} & 0 \\ \varepsilon_{yx} & \varepsilon_{yy} & 0 \\ 0 & 0 & \varepsilon_{zz} \end{bmatrix}, \quad \varepsilon_{xx} = \varepsilon_{yy} \quad (8)$$



The computer program and formulae used in the paper cited above by Alpert, Budden, etc. [4] for numerical calculations of the moduli  $|\mathbf{E}|$  was developed by K. Budden. The first order descents evaluation of the integrals used by these calculations give the contribution of the saddle points of the Axis and of the both Storey and Reversed Storey cone fields.

The field  $E_0$  is expressed by an algebraic combination of the both Bessel functions  $J_0(n_\perp, \rho)$  and  $J_1(n_\perp, \rho)$  (see (5)), and also by a combination of the components of the refraction index  $\mathbf{n}$  and of the elements of the tensor  $\varepsilon_0$  of the plasma. The fields  $|\mathbf{E}_{\text{St}}|$  and  $|\mathbf{E}_{\text{RevSt}}|$  are expressed by a combination of the Airy integral function  $A_i(p)$  and its derivative  $A'_i(p)$ , and also by  $\mathbf{n}$  and  $\varepsilon_0$ . The field in the resonance cone  $|\mathbf{E}_{\text{Res}}|$  is much simpler and is expressed by an algebraic combination of the elements of the tensor, and of the refraction index  $\mathbf{n}$ . Certainly, all these formulae depend on the angular frequencies  $\omega$  and the angle of the ray direction  $\beta$ .

The general formulae of  $|\mathbf{E}|$  and the formulae used by the programming are complicated. For orientation, only schematical formulae were given here. They show the distance and angle dependence of the moduli of the field interesting for us in this study

$$|\mathbf{E}| = \left( |E_x|^2 + |E_y|^2 + |E_z|^2 \right)^{1/2}. \quad (9)$$

These asymptotic formulae are of the following shape:

The Axis field

$$|\mathbf{E}_0| \simeq \left( I \frac{\omega^3}{c^3} \right) n_\rho^2 \left( \frac{2\pi n_z}{\frac{\omega}{c} z} \right)^{1/2} \cdot \exp \left[ -i \left( \frac{\omega}{c} z n_z \pm \frac{\pi}{4} \right) \right] \cdot F_{Ax}[J_0, J_1, \mathbf{n}, \varepsilon_0], \quad (10)$$

where all the values of  $F_{Ax}[\dots]$  depend on  $\omega$ ,  $\beta$  and on the characteristics frequencies of the magnetoplasma.

The field in the two Storey cones

$$|\mathbf{E}_{St}| \simeq \left( I \frac{\omega^3}{c^3} \right) \cdot \frac{\sqrt{\pi} \cdot \exp(-i\{\dots\})}{\left( \frac{\omega}{c} r \right)^{5/6} \cdot (\cos \beta)^{1/3} \cdot (\sin \beta)^{1/2}} \cdot F_{St}[A_i(p), A'_i(p), \mathbf{n}, \varepsilon_0], \quad (11)$$

where all the values of  $F_{St}[\dots]$  depend on  $\omega$ ,  $\beta$ , etc.,  $A_i(p)$  and  $A'_i(p)$  are the Airy function and its derivative,

$$p = \left( \frac{dn_{\parallel}}{dn_{\perp}} + \frac{\rho}{z} \right) \cdot \left( \frac{2}{n_{\parallel}} \right)^{1/2} \cdot \left( \frac{\omega}{c} z \right)^{2/3}, \quad (12)$$

and  $F_{St}\{\dots\}$  is determined by some parameters of the magnetoplasma, by  $\omega$  and  $\beta$ .

The field in the Resonance cone

$$|\mathbf{E}_{Res}| \simeq \left( I \frac{\omega^3}{c^3} \right) \cdot \frac{n_\rho n_z \exp \left[ -i \frac{\omega}{c} r (n_\rho \sin \beta + n_z \cos \beta) \right]}{\left( \frac{\omega}{c} r \right)} \cdot F_{Res}[\mathbf{n}(\omega, \beta), \varepsilon_0(\omega, \beta), \beta]. \quad (13)$$

## II.2 Frequency and angle dependencies of $|\mathbf{E}|$ in all the regions of their enhancement and focusing.

The structure of the electromagnetic field in a full ionized and homogeneous magnetoplasma discussed here was initially studied by detailed investigations of the behavior of the direction of the group velocity vector  $\mathbf{U} = d\omega/d\mathbf{k}$  in a magnetoplasma. Namely the dependence of the angle  $\beta$  between the vectors  $\mathbf{U}$  and  $\mathbf{B}_0$  on the angle  $\Theta$  between the wave vector  $\mathbf{k}$  and  $\mathbf{B}_0$  reveals the basic features of the field and permits to determine the characteristic frequencies and angles of these phenomena (see [2]). This is explained by the following.

The vector  $\mathbf{U}$  and the pointing vector  $\mathbf{S}$  are collinear in an non-absorbing plasma (see [6]). This theorem may be used in a weakly absorbing plasma, which is namely our case because the collision frequency  $\nu$  in the discussed here regions of the plasma is very small (see below). Let us illustrate here briefly the behavior of  $\beta(\Theta)$  in connection and in limits of the present study by the following two figures.

On Fig.1 the dependence of  $\beta$  on  $\Theta$  is shown. It is determined by

$$\beta = \Theta - \arctan \left( \frac{1}{n} \cdot \frac{\partial n}{\partial \Theta} \right), \quad (14)$$

where  $n = n(\Theta, \varepsilon, \omega)$  is the coefficient of refraction of the magnetoplasma. By calculation of  $\beta(\Theta)$  given of Fig.1 and of different dependencies of the electric field given in this section, we used the following model of a magnetoplasma,

consisting only of one kind of ions (namely protons  $H^+$ ):

$$\begin{aligned} f_0 &= 3.39 \cdot 10^6 \text{ Hz}, \quad f_b = 1.194 \cdot 10^6 \text{ Hz} \quad F_L = 2.49 \cdot 10^4 \text{ Hz}, \\ \nu_{ei} &= 10^2 \text{ sec}^{-1}, \quad \frac{m}{M_{H_1}} = 5.44 \cdot 10^{-4}, \end{aligned} \quad (15)$$

where  $f_0$  and  $f_b$  are the electron Lengmuir and gyro- frequencies,  $\nu_{ei}$  is the electron-ion collision frequency,  $m$  and  $M_{H_1}$  are the electron and proton masses. This model is close to the parameters of the plasma in the vicinity of the maximum of the ionosphere. Namely this figure and Fig.2, where a schematic frequency dependence of the coefficient of refraction  $n$  is given, demonstrate the distribution of the angles and the characteristic frequencies of the cones formed in a magnetoplasma in the **VLF** and **LF** frequency bands, shown on Fig.1.

The generatrix of the Storey cones, shown on Fig.1 contains the maxima angles  $\beta_M$  of the angle dependencies  $\beta(\Theta)$ . The maximal value of  $\beta_{M,max} = \beta_{St,M}$ . It corresponds to the upper frequency limit  $\omega_{RS}/\omega_b$ , ( $\omega_{RS} = 2\pi F_{RS}$ ), where the Storey cones and Reversed Storey cones disappear. It is determined by the point of inflection of  $\beta(\Theta)$ . The generatrix of the Reversed Storey cones contains the angles  $\beta_m$  of the minima of  $\beta(\Theta)$ . The upper frequency limit of  $\beta_{m,max} = \beta_{M,max}$  also corresponds to  $\omega_{RS}/\omega_b$ , where both the maxima and minima of  $\beta(\Theta)$  approach each other and disappear. The low frequency limits of the Storey and Reversed Storey cones correspond to  $\omega_{S2}/\omega_b$  and  $\omega_L/\omega_b$  ( $\omega_{S2} = 2\pi F_{S2}$ ), where again the maxima and minima of  $\beta(\Theta)$  disappear (see Figs. 1 to 3). Thus, the frequency bands of the Storey and Reversed Storey cones respectively are: ( $\omega_{RS}$  to  $\omega_{S2}$ ) and ( $\omega_{RS}$  to  $\omega_L$ ),

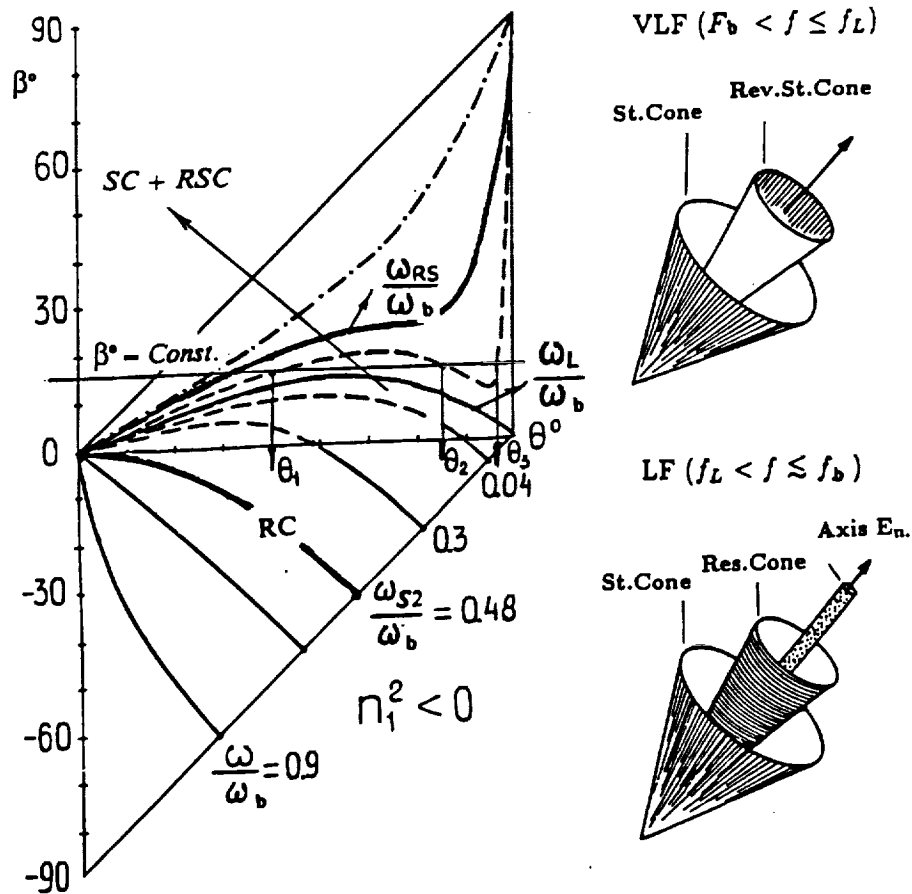


**Fig 1.** The dependence of the angle  $\beta$  between the group velocity  $U$  and the magnetic field  $B_0$  on the angle  $\theta$  between the wave number vector  $k$  and  $B_0$ .

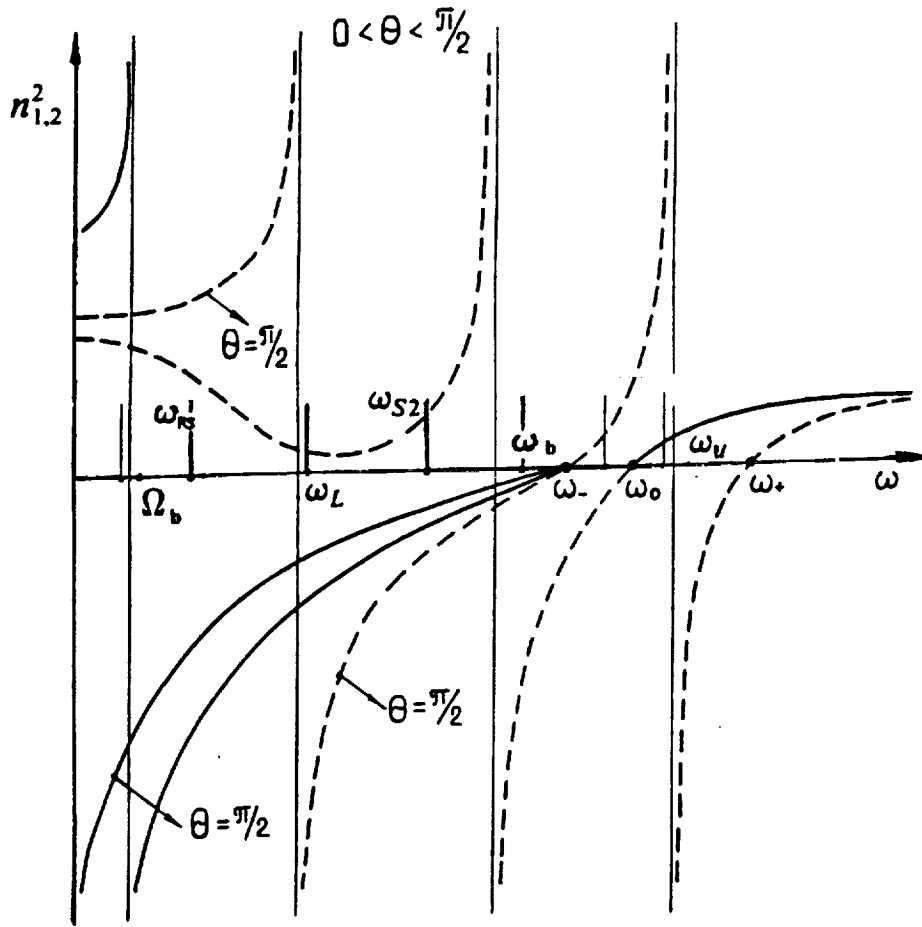


**Fig 2.** The coefficient refraction  $n$  depending on the angular frequency  $\omega = 2\pi F$  or  $\omega = 2\pi f$ .

the frequency  $\omega_{RS} \ll \omega_L$ . In the model of the magnetoplasma used in this section (see (15)) these characteristic frequencies  $F$  and the characteristic angles  $\beta$  of both of the Storey cones are equal to:

$$\begin{aligned} F_{St,Max} &= \frac{\omega_{RS}}{2\pi} = 2.6 \cdot 10^{-3} \text{ Hz} , \quad \beta_{St,Max} = 21^\circ; \\ F_{St,0} &= \frac{\omega_{S2}}{2\pi} = 0.48 f_b \text{ Hz} , \quad \beta_{St,0} = 0^\circ; \\ F_{Rev.St,0} &= \frac{\omega_L}{2\pi} = 2.087 \cdot 10^{-2} \text{ Hz} , \quad \beta_{Res.St,0} = 0^\circ \end{aligned} \quad (16)$$

The resonance cones are formed in the frequency band ( $F_L$  to  $f_b$ ) and in the angle region (0 to  $90^\circ$ ).

Angular dependencies of the electric field in different cones and of the Axis field at different frequencies ratios  $F/f_b$  are shown on Figs.3 and 4. It is natural that the Axis field and the fields inside both Storey cones are oscillating because they are formed by superposition of two modes (mathematically by contribution of the saddle points, see above section II.1). The maximal values  $Max|\mathbf{E}|_{max}$  of  $|\mathbf{E}|_{max}$  of these oscillations of the Axis field and Reversed Storey cones are closer to the direction of  $\mathbf{B}_0$ . They are determined below by the notation  $\beta_{max}$ . The resonance field has only one maximum. It is formed only by one saddle point and it is also denoted by  $\beta_{max}$ .

Let us note here that the notations  $Max|\mathbf{E}|_{max}$  both of  $|\mathbf{E}_0|_{max}$ ,  $|\mathbf{E}_{Rev.St}|_{max}$ ,  $|\mathbf{E}_{St}|_{max}$  and of  $|\mathbf{E}_{res}|_{max}$  are used below in this and in the following sections. The given below values of  $\beta$  on the plots and in the tables are also the values  $\beta_{max}$  of these fields.

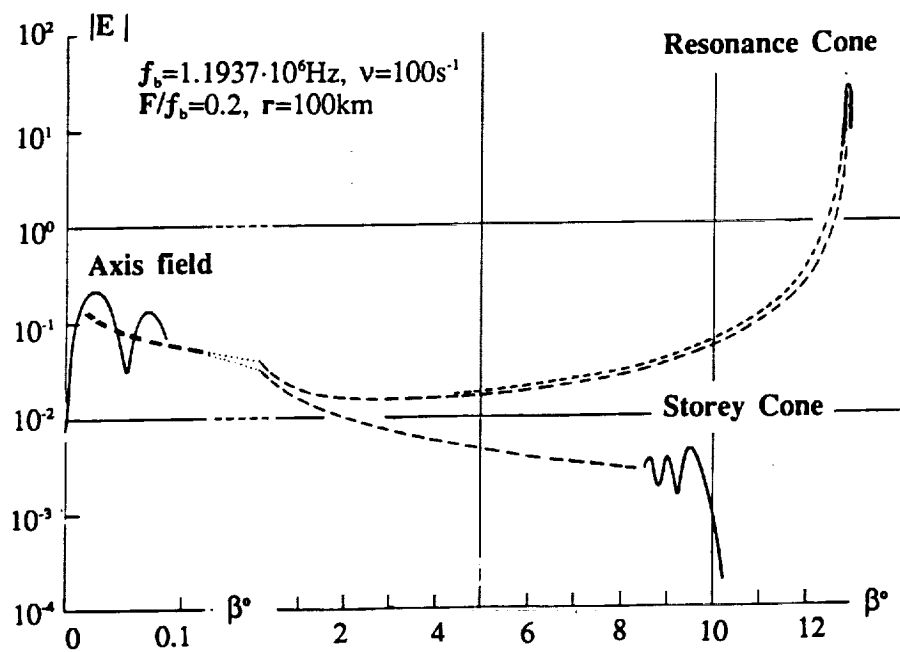


**Fig 3.** Angular dependencies of  $E$ .



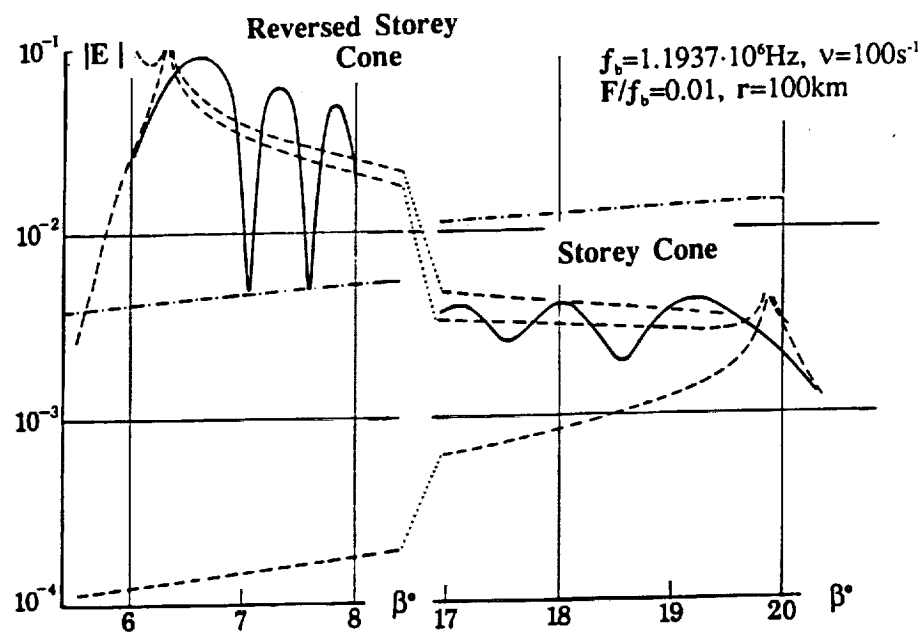


**Fig 4.** Angular dependencies of  $E$ .

Frequency dependencies  $\delta_{Max}|\mathbf{E}_0|_{max}$  namely of the normalized maximum values of the Axis fields  $|\mathbf{E}_0|_{max}$ ,  $|\mathbf{E}_{St}|_{max}$ ,  $|\mathbf{E}_{Rev.St}|_{max}$  and  $|\mathbf{E}_{Res}|_{max}$  are given on Fig.5 and in the Table I. The values of  $|\mathbf{E}|$  were normalized to the field of the Storey cone  $|\mathbf{E}_{St}|_{max}$  in the frequency band  $F/f_b = (0.01 \text{ to } 0.2)$  because in this frequency band  $|\mathbf{E}_{St}|_{max}$  is almost a constant; it is changing very slowly.

The values of  $\beta$  of the Storey cones are changing in the frequency band  $F/f_b \sim 0.1 \text{ to } 0.28$  from  $\beta_{max} = 21^\circ$  up to  $8.9^\circ$ , and  $\beta_{max} \rightarrow 0^\circ$ , when  $F/f_b = 0.48$  (see Fig.5). The amplitudes of the electric field  $|\mathbf{E}_{St}|_{max}$  are in reall conditions about  $(10 \text{ to } 10^2)$  and more times larger than the electric field in the free space, however, much smaller than the Axis field and the field in the other cones.

The enhancement of the field by approaching the low hybrid frequency is absent in the Storey cone because it is formed, simply speaking, only by the oscillations of the electrons and depends very little on the oscillations of ions which produce the low hybrid resonance and the Reversed Storey cone. In the earlier studies, by discussing the guiding of **LF** waves, i.e. of the electron whistlers, along  $\mathbf{B}_0$ , the influence of the ions was not taken into account. Therefore, the formation of the Reversed Storey cone, was omitted.

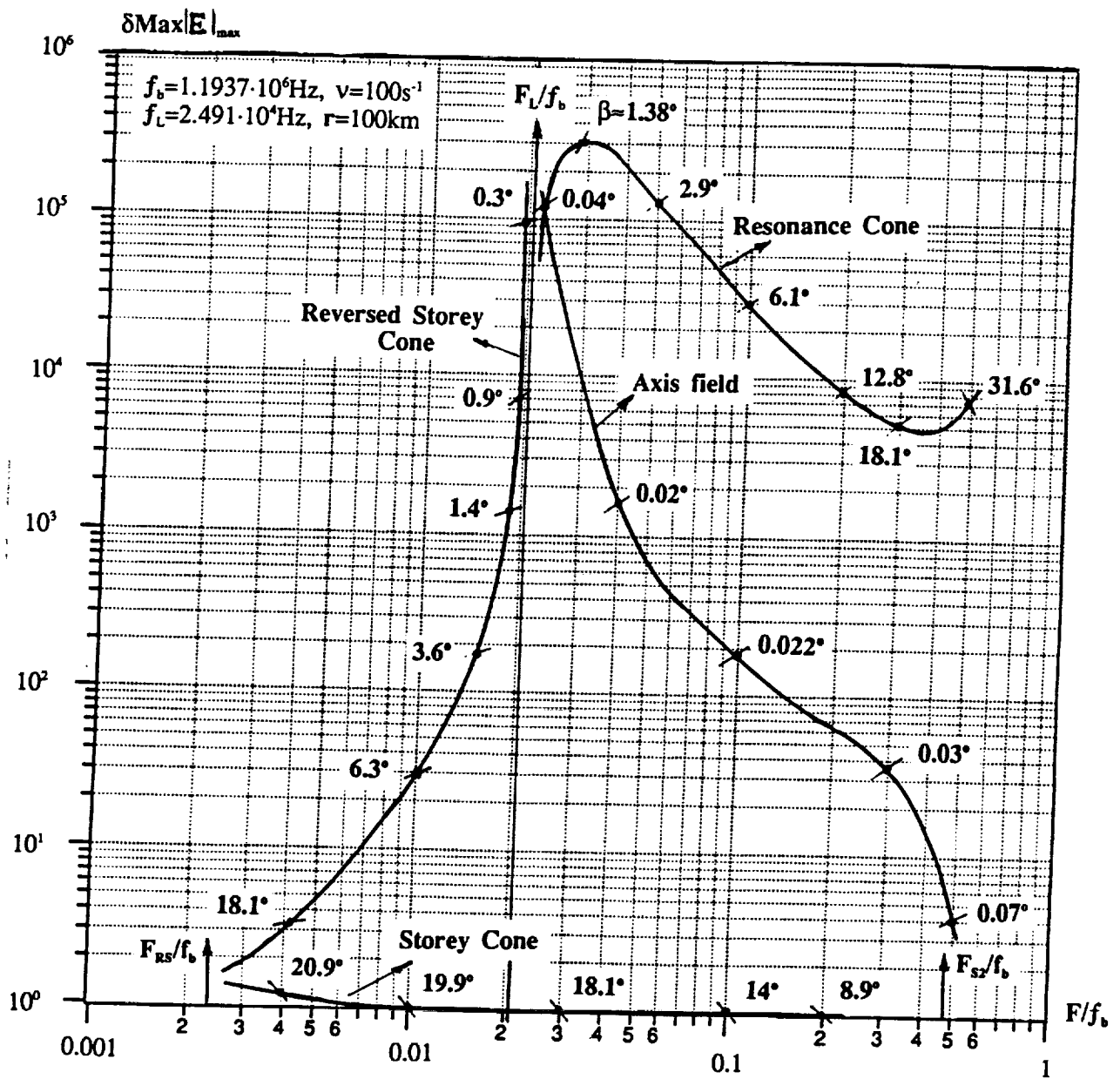


Fig 5. Normalized frequency dependencies of the moduli of the electric field.  
 The numbers near curves are the values of  $\beta_{\text{max}}$ .

**Table I.** Normalized values  $\delta_{Max}|E|_{max} = Max|E|_{max}/Max|E_{St}|_{max}$ .

$F/f_b$	St.C.	Rev.St.C.	Axis field	Res.C.
<b>0.003</b>	1.2	1.9	-	-
<b>0.005</b>	$\sim 1$	4.8	-	-
<b>0.008</b>	$\sim 1$	19	-	-
<b>0.01</b>	$\sim 1$	24	-	-
<b><math>1.88 \cdot 10^{-2}</math></b>	$\sim 1$	1502	-	-
<b><math>\sim 0.02</math></b>	$\sim 1$	-	$2.4 \cdot 10^5$	$1.4 \cdot 10^5$
<b>0.03</b>	$\sim 1$	-	$1.9 \cdot 10^4$	$3.1 \cdot 10^5$
<b>0.05</b>	$\sim 1$	-	670	$1.1 \cdot 10^5$
<b>0.1</b>	$\sim 1$	-	215	$3 \cdot 10^4$
<b>0.3</b>	0.47	-	36	$5.1 \cdot 10^3$
<b>0.5</b>	0.024	-	4	$8 \cdot 10^3$

By consideration of Fig.5 it follows that both the Axis field and the fields in the Reversed Storey and Resonance cones are very large and grow up very quickly, especially by approaching the low hybrid frequency  $F_L$ . The maximum values of  $|E|$  become in this region about  $10^5$  times larger than in the Storey cone and the directions (angles  $\beta_{max}$ ) of the maximum values of  $|E|$  become closer to the direction of the magnetic field  $\mathbf{B}_0$ . The apexes of the cones, where the most part of flux of the field is concentrated, become very narrow. This is shown in the next section in more detail, by presenting the results of calculation of  $|E|$  at high altitudes of the ionosphere and in the magnetosphere.

### III. The electric field $|\mathbf{E}|$ at $Z = (800 - 6000)km$ .

The altitude behavior of the electric field in the ionosphere and magnetosphere is presented in this section by detailed calculations of the Axis field  $|\mathbf{E}_0|$  and resonance field  $|\mathbf{E}_{res}|$ . By calculation of  $|\mathbf{E}|$ , both in this and in the previous sections, the factor  $(\frac{\omega^3}{c^3})$  is omitted (see formulae (10) to (13)). This factor is used on the dependencies shown on Fig.5 and 14 by normalization of  $|\mathbf{E}|$  and by comparison of  $|\mathbf{E}_0|$  and  $|\mathbf{E}_{res}|$ . Both the oscillating character of  $|\mathbf{E}_0|$ , depending on the horizontal distance  $x = r \tan \beta_{max}$  from the Axis  $z$ , which is parallel to  $\mathbf{B}_0$  and of  $|\mathbf{E}_{res}|$ , depending on the angle  $\beta$ , and also their frequency dependencies are examined in this section.

#### III.1 Altitude and angle dependencies of $|\mathbf{E}_0|$ and $|\mathbf{E}_{Res}|$ .

The preliminary calculations have shown that the amplitude of  $|\mathbf{E}|$  is growing up very quickly in the altitude region  $Z = (400 \text{ to } 800)km$ . In this altitude region the values of the electric field are also very small. For example, at  $Z = (400, 500, 800, 1000)km$  the maximum values of  $|\mathbf{E}_0|$  of the Axis field are equal to

$$Max|\mathbf{E}_0|_{max} \simeq 6.6 \cdot 10^{-2}, 2.9, 9.5 \cdot 10^2, 1.4 \cdot 10^5; \quad (17)$$

and at  $Z = (800, 1000)km$ , the values  $Max|E_{res}|_{max} \simeq 28$  and 1887. I.e. the effect of the enhancement of the flux of **VLF** and **LF** electromagnetic waves in the Earth magnetoplasma, caused by the *caustic focusing*, is especially pronounced at high altitudes. Therefore, we discuss here only the behavior

of the field  $|\mathbf{E}|$  at  $Z \geq 800 \text{ km}$ .

By these calculations we used the model of the ionosphere and magnetosphere given in Table I. This model is nearly conformed to day-time middle latitude conditions. The notations used in the table are the following:

$Z$  is the altitude above the Earth's surface,  $N_n$  and  $N_{e,i}$  are the densities of the neutral particles, electrons and ions;

$T^\circ, K$  and  $B, \gamma$  are the temperature in Kelvin degrees and the magnetic field in gammas  $\gamma(nT)$  along the Earth's magnetic field line;

$\nu_{en}$  and  $\nu_{ei}$  are the collision frequencies between the electrons and the neutral particles and the ions;

$f_0$  and  $F_0$  are the Lengmuir plasma frequencies of the electrons and ions;

$f_b, F_b, F_L$  are the electron's and ion's gyro-frequencies and the low hybrid frequency of the ions

$$F_L = \left( \frac{f_b F_b}{1 + \frac{f_b^2}{f_0^2}} \right)^{1/2}. \quad (18)$$

Up to the altitude about  $(800 - 1000) \text{ km}$  the ionosphere consists of a noticeable number of Oxygen and Helium ions ( $O_1^+$  and  $He^+$ ) including protons  $H_1^+$ . Therefore, in the lower part of the ionosphere, by calculations of the electron and ion gyro-frequencies  $f_b$  and  $F_b$ , the effective mass of the neutral particles is used:

$$M_{eff} = M_{H_1} \left( \sum_{s=1,2,3} \frac{N_{is}}{N_{ei}} \cdot \frac{M_{H_1}}{M_{is}} \right)^{-1}, \quad s = 1, 2, 3. \quad (19)$$

Table II. Parameters of the ionosphere.

$Z, km$	400	500	800	1000	1500	2000	2500	3000	4000	6000
$N_n, cm^{-3}$	$5 \cdot 10^8$	$5 \cdot 10^7$	$2 \cdot 10^6$	$4 \cdot 10^5$	$6 \cdot 10^3$	$2 \cdot 10^3$	20	$< 1$	$\sim 0.2$	$\ll 1$
$N_e \cdot 10^{-3}, cm^{-3}$	1500	1000	400	230	70	20	10	8	6	5
$M_{eff}^+/M_{H1}^+$	3	2	1.2	1	1	-	-	-	-	-
$T, K^\circ$	1800	1800	1800	2000	2500	3000	3500	4000	4500	5000
$B_0 \cdot 10^{-4}, \gamma$	4.15	3.96	3.52	3.24	2.66	2.21	1.82	1.55	1.15	0.68
$\nu_{en}, s^{-1}$	6	0.7	$3 \cdot 10^{-2}$	$8 \cdot 10^{-3}$	$6 \cdot 10^{-4}$	-	-	-	-	-
$\nu_{ei}, s^{-1}$	1500	700	150	40	20	7	2	1.5	1	0.7
$f_o \cdot 10^{-6}, Hz$	11.0	8.98	5.08	4.31	2.38	1.27	0.898	0.82	0.71	0.63
$F_o \cdot 10^{-4}, Hz$	14.8	14.8	12.1	10.1	5.55	2.96	2.09	1.91	1.65	1.45
$f_b \cdot 10^{-5}, Hz$	11.62	11.1	9.87	9.07	7.45	6.21	5.09	4.34	3.21	1.91
$F_b \cdot 10^{-2}, Hz$	2.1	3.02	4.47	4.93	4.05	3.38	2.77	2.36	1.74	1.04
$F_L \cdot 10^{-3}, Hz$	15.53	18.17	20.61	20.69	16.58	13.05	10.33	8.89	6.79	4.27

In (19),  $N_{is}$  and  $M_{is}$  are, respectively, the ion densities and masses of  $H_1^+$ ,  $He^+$  and  $O_1^+$ . For fixed altitudes  $Z$ , the results of these calculations of  $|E_0|$  are presented on Figs. 6 to 9, and of  $|E_{res}|$  on Figs. 10 to 13. The main characteristics of these fields are given in the Tables III and IV.

**Table III. Data of the Axis field  $|E_0|$ .**

<b>Z , km</b>	<b><math>(F_L/F_b) \cdot 10^2</math></b>	<b><math>(F_{max}/F_b) \cdot 10^2</math></b>	<b><math>F_{max}</math> , kHz</b>	<b>Max<math> E_0 _{max}</math></b>
<b>800</b>	2.088	2.297	22.60	951
<b>1000</b>	2.281	2.2831	20.71	$1.38 \cdot 10^5$
<b>1500</b>	2.226	2.2266	16.59	$2.17 \cdot 10^6$
<b>2000</b>	2.101	$\sim 2.1$	13.02	$1.58 \cdot 10^7$
<b>2500</b>	2.029	2.030	10.33	$8.285 \cdot 10^7$
<b>3000</b>	2.048	2.062	8.951	$1.116 \cdot 10^8$
<b>4000</b>	2.115	2.126	6.825	$1.557 \cdot 10^8$
<b>6000</b>	2.236	2.2345	4.264	$2.109 \cdot 10^8$

**Table IV. Data of the resonance field  $|E_{res}|$ .**

<b>Z , km</b>	<b><math>F/F_{max}</math></b>	<b><math>F_{max}</math> , kHz</b>	<b>Max<math> E_0 _{max}</math></b>	<b><math>\beta_{max}</math> , deg</b>
<b>800</b>	0.03	29.6	27.7	$\sim 1.12$
<b>1000</b>	0.0285	25.85	1937	0.0998
<b>3000</b>	0.0220	9.548	$1.157 \cdot 10^7$	0.496
<b>6000</b>	0.0240	4.584	$2.449 \cdot 10^7$	0,527



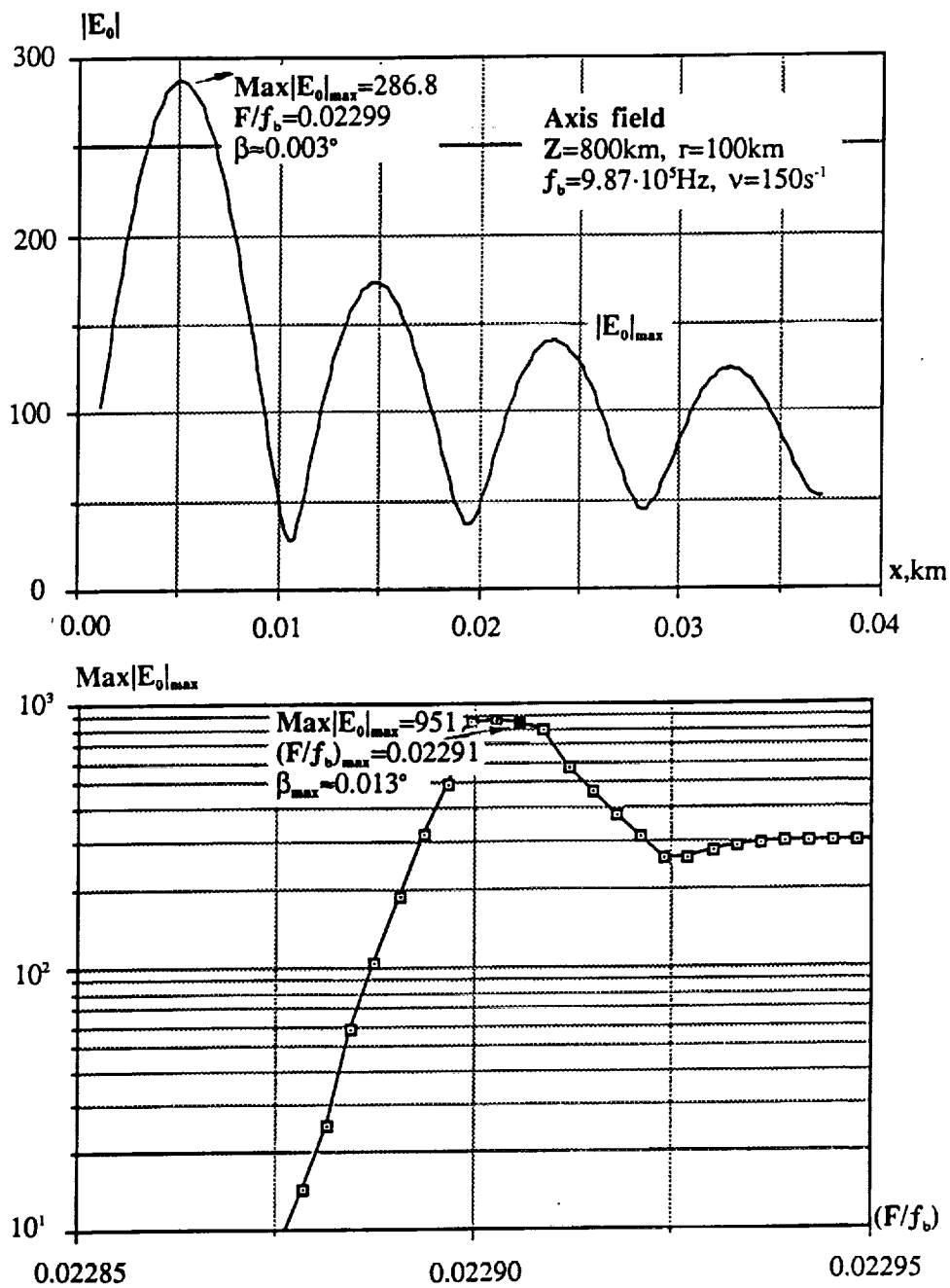


Fig 6. The field  $|E_0|$  of the Axis

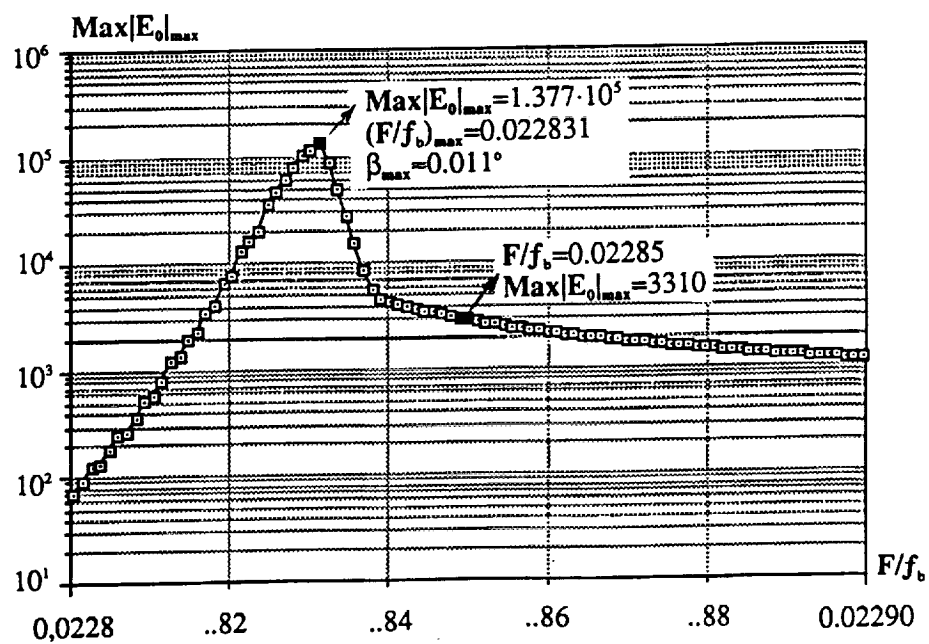
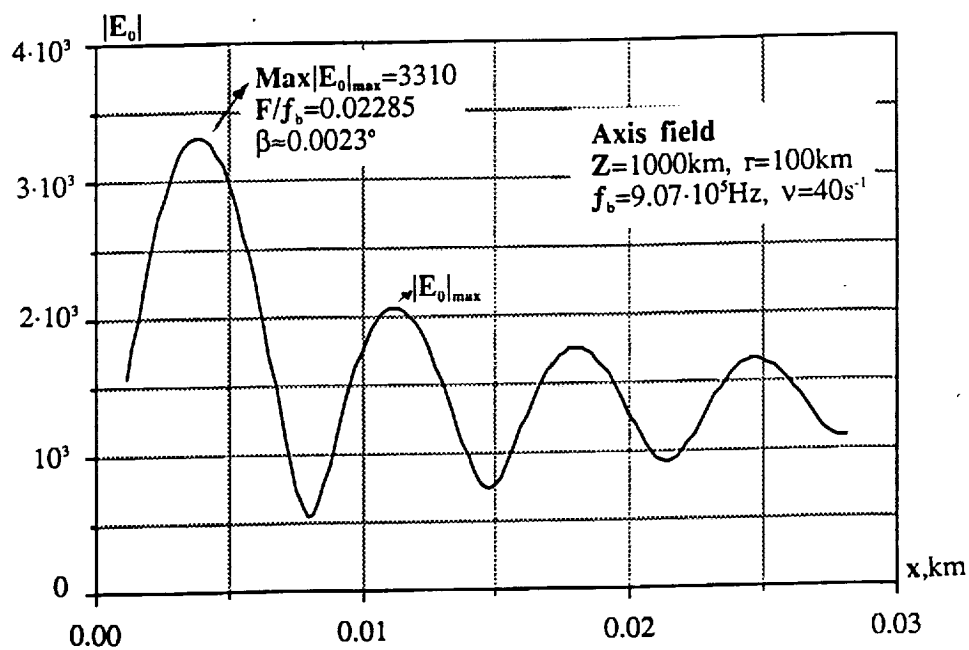


Fig 7. The field  $|E_0|$  of the Axis

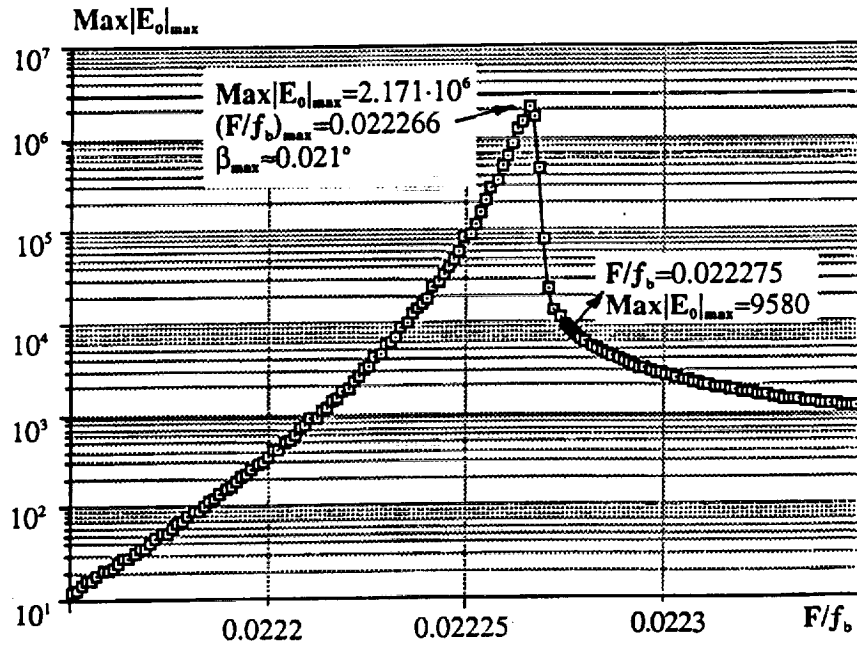
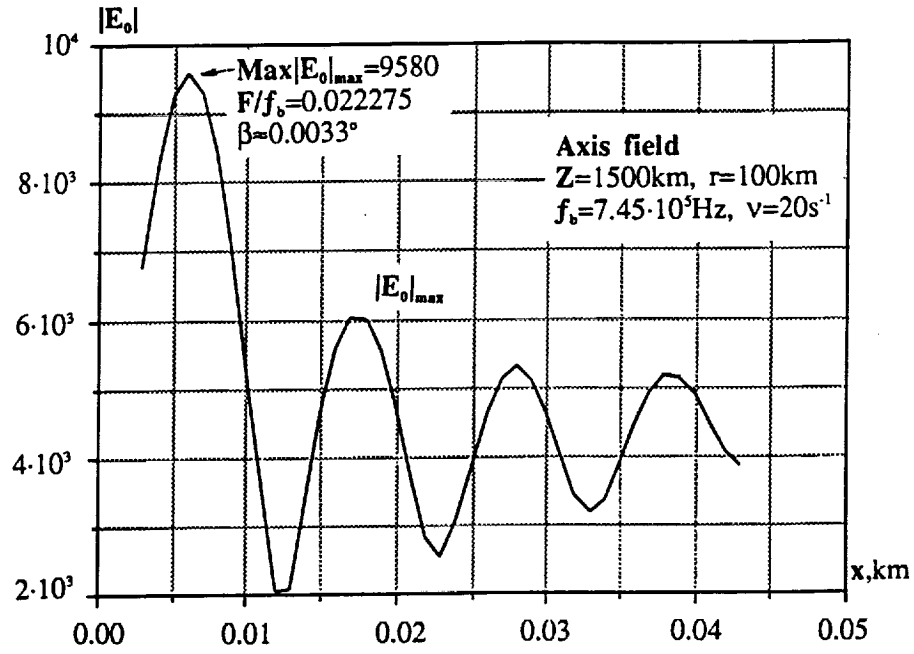
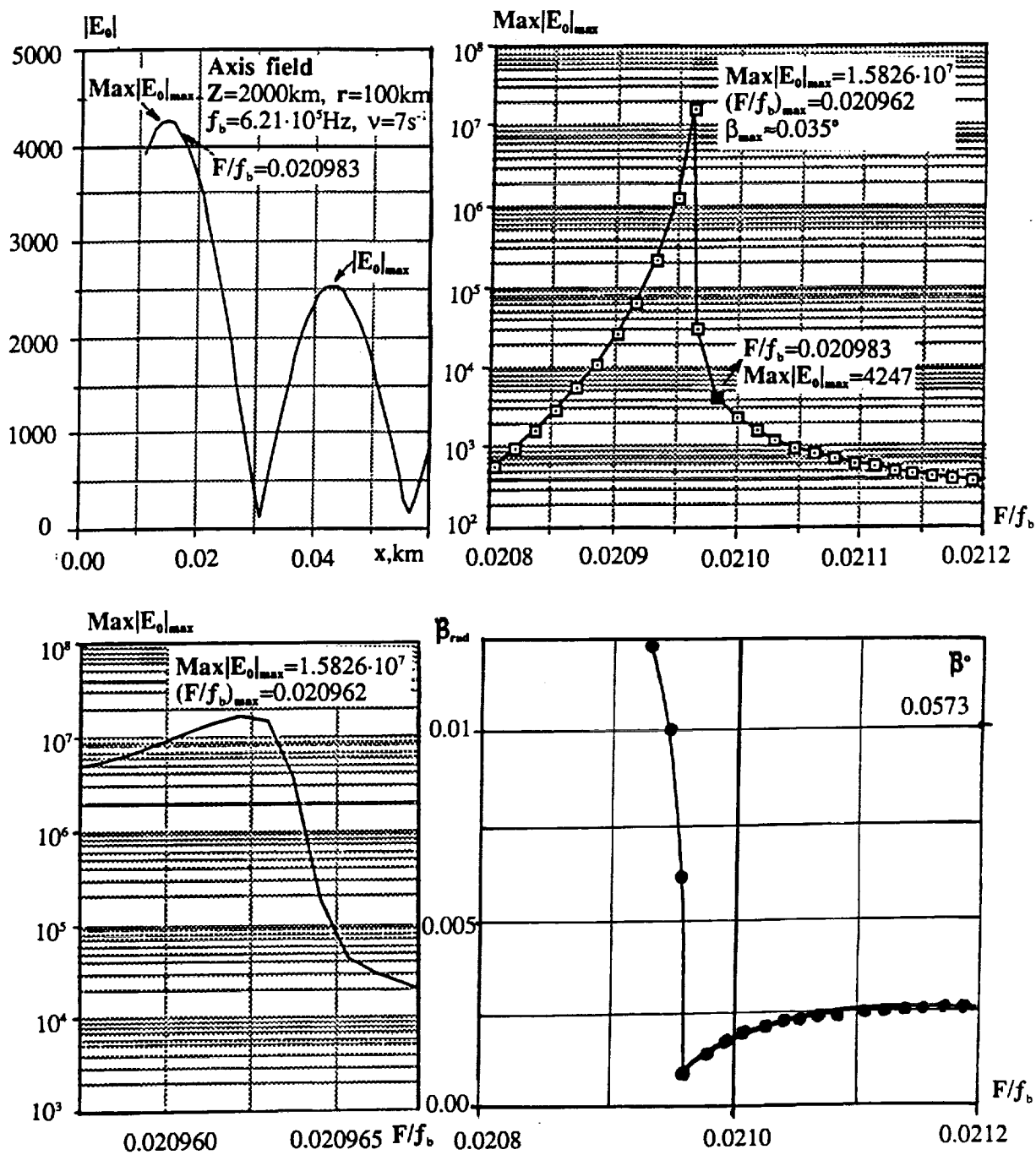


Fig 8. The field  $|E_0|$  of the Axis



**Fig 9.** The field  $|E_0|$  and the frequency dependence of  $\beta$  of the Axis field.

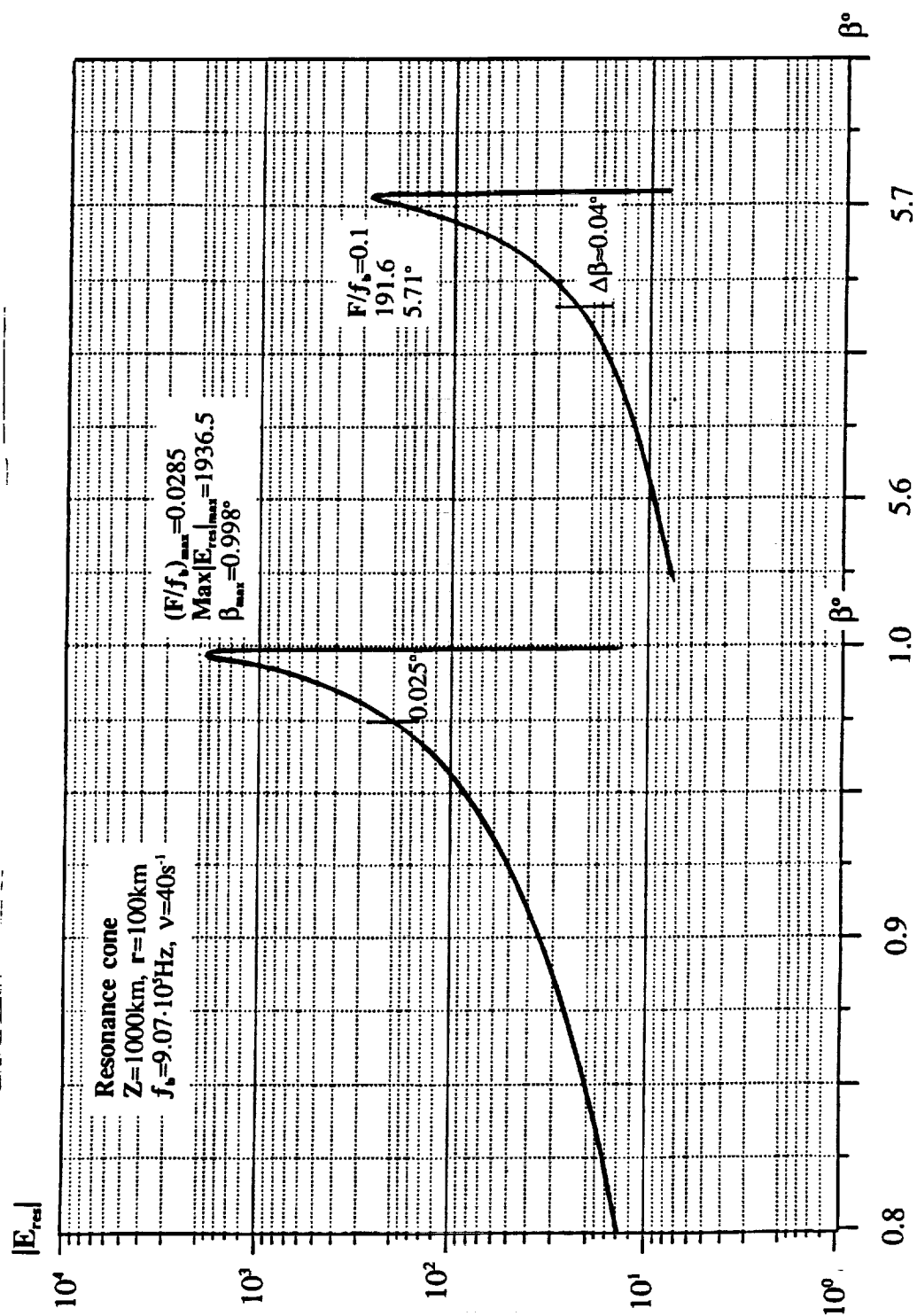


Fig 10. Angle dependencies of  $|E_{\text{res}}|$ .

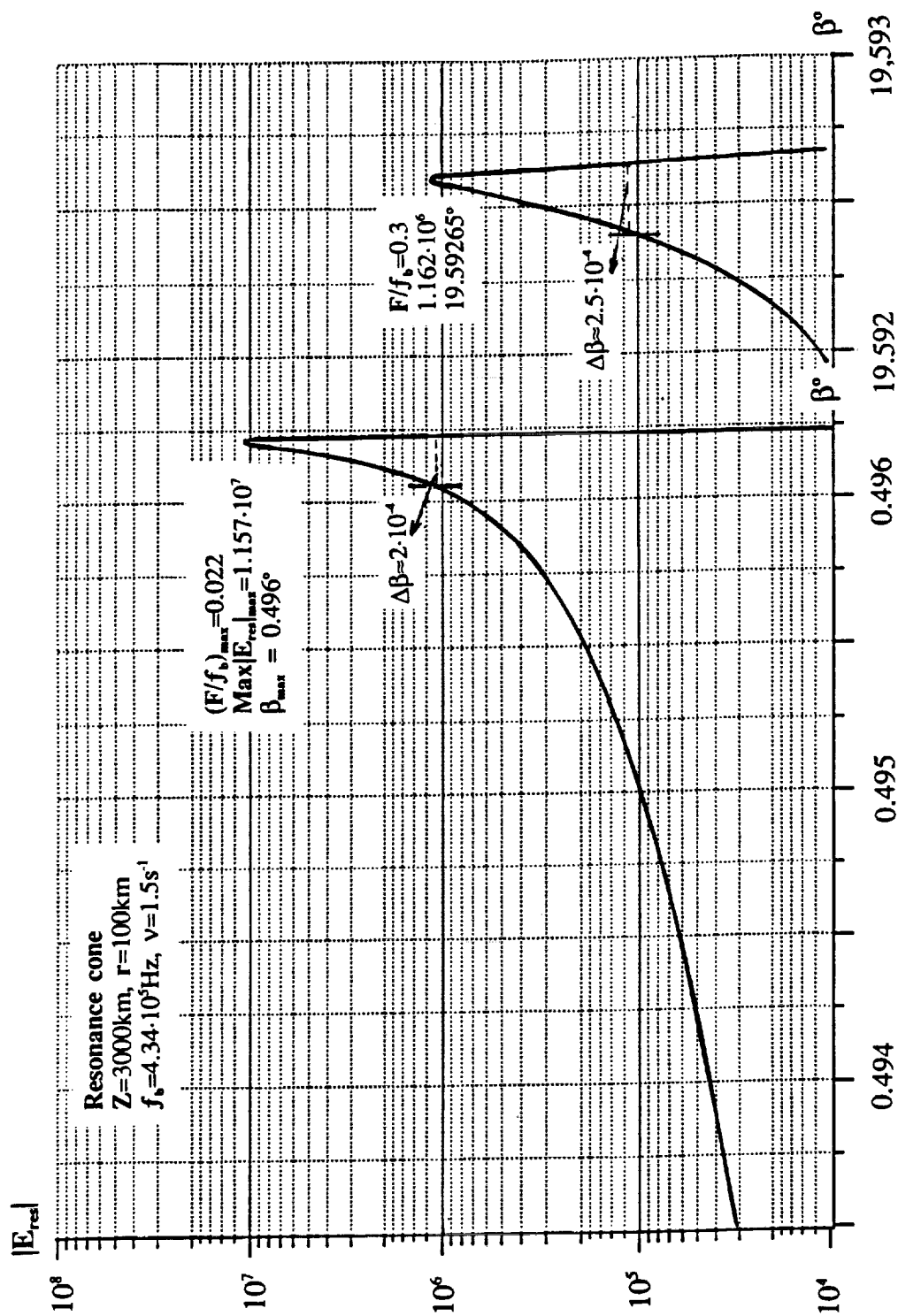


Fig 11. Angle dependencies of  $|E_{\text{res}}|$ .

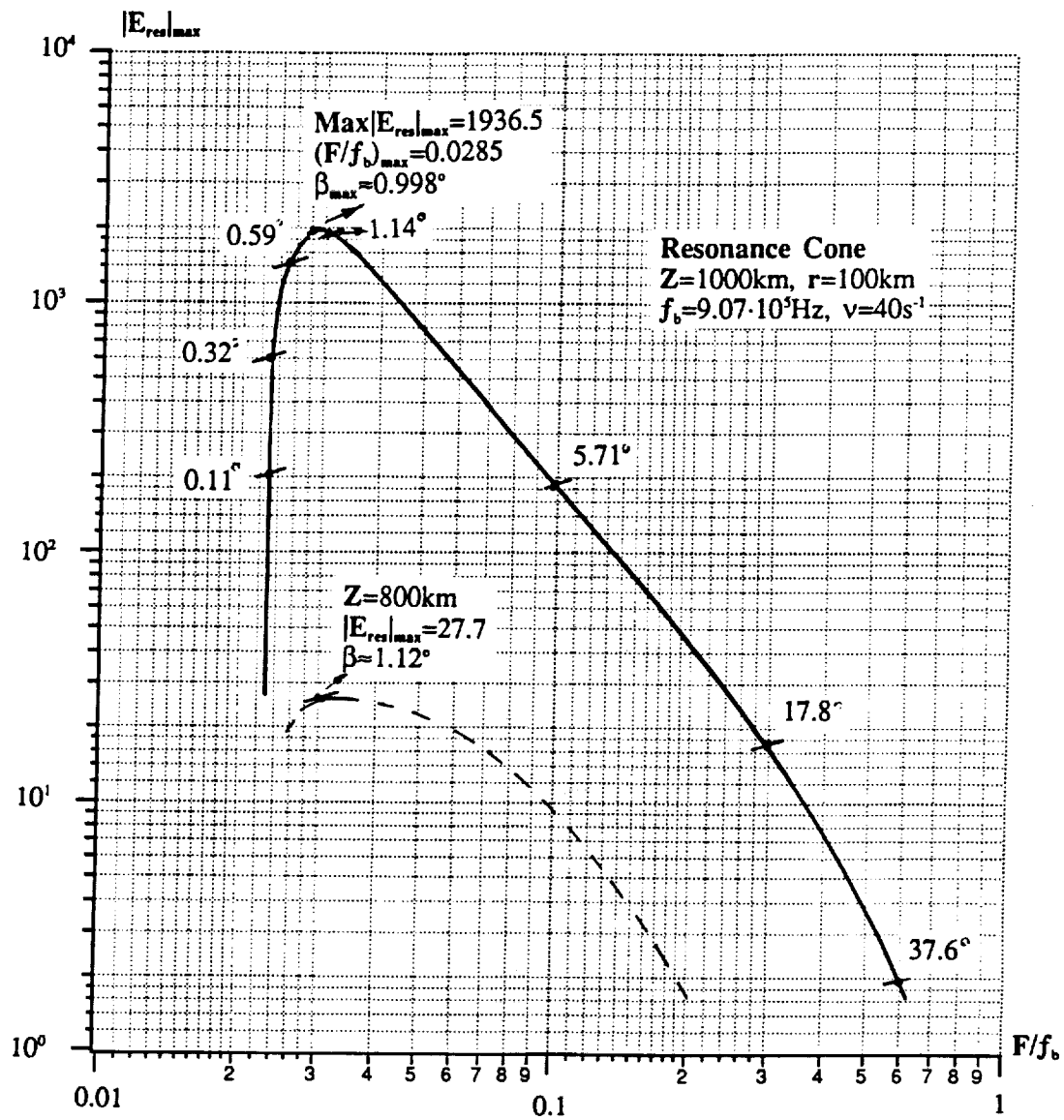


Fig 12. Frequency dependencies of  $|E_{res}|$ .

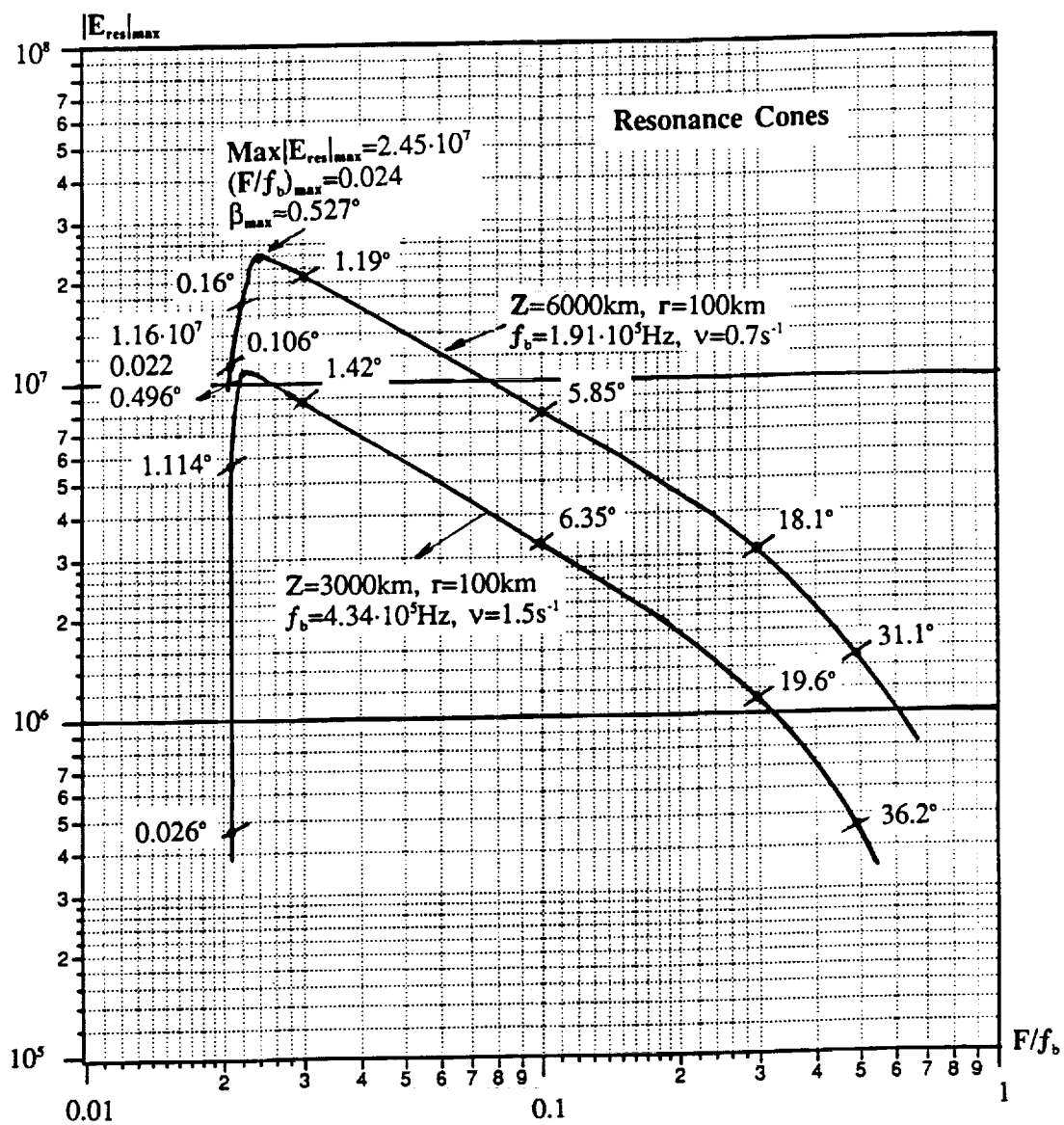


Fig 13. Frequency dependencies of  $|E_{res}|$ .



### III.2 Discussion of the principal properties of $|\mathbf{E}|$ .

The dependencies of  $|\mathbf{E}_0|$  on  $x$  and of  $Max|\mathbf{E}_0|_{max}$  on  $F/f_b$  shown on Figs.(6 to 9) demonstrate the following main features of the Axis field: its oscillating character by moving away from the magnetic field line  $\mathbf{B}_0$  ( $\beta = 0$ ) and the very pronounced maximum of  $Max|\mathbf{E}_0|_{max}$  of the electric field  $|\mathbf{E}_0|$  depending on  $F/f_b$ . Besides, the  $Max|\mathbf{E}_0|_{max}$  is the closest to the line  $\mathbf{B}_0$  and is characterized by the angle  $\beta_{max} = \arctan x/r$ . These angles are very small, they grow up with altitude, for example, as the following

$$Z, km = 800, 1000, 1500, 2000, 2500 \quad (20)$$

$$\beta, deg = 0.014, 0.02, 0.04, 0.06, 0.07$$

The frequency dependence  $\beta(F)$  has a minimum which is a little shifted from the frequency  $F_{max}$  and  $\beta(F)$  is growing up by approaching the low hybrid frequency  $F_L$  (see Fig.9). The dependence of  $Max|\mathbf{E}_0|_{max}$  on frequency in the neighborhood of  $F = F_{max}$  is also given on this figure. A very important characteristic of the frequency dependence of the Axis field is its *narrow-band character* of the value  $F_{max}$  in the vicinity of  $Max|\mathbf{E}_0|_{max}$ . Namely, about 99% of the flux of these electromagnetic waves are concentrated at the altitudes  $Z = (800 \text{ to } 6000)km$  discussed here in the frequency band

$$\Delta F_{max} \sim (2 \cdot 10^{-3} \text{ to } 9 \cdot 10^{-4}) F_{max} \quad (21)$$

The behavior of both the electric fields  $|\mathbf{E}_{res}|$ , shown in detail on Figs. (10 to 14) and of  $|\mathbf{E}_{St}|$  and  $|\mathbf{E}_{Rev.St.}|$ , (see Figs. (3 to 5)), differs, in many respects, from the behavior of the Axis field  $\mathbf{E}_0$ . The frequency dependencies

of the maxima of these fields have also pronounced maxima at  $\mathbf{F}_L$ . However,  $\beta_{max}$  is changing considerable with frequency (see Figs. 5, 12, 13). For example, at  $F/f_b = ((F/f_b)_{max}, 0.03, 0.1, 0.3, 0.5)$ , the values  $|\mathbf{E}_{res}|_{max}$  are conformed to the following values of  $\beta_{max}$ :

$$Z = 1000 \text{ km} : \beta_{max} = 0.998 \quad , \quad 1.14, 5.7, 17.8, 37.6 \quad (22)$$

$$Z = 3000 \text{ km} : \beta_{max} = 0.496 \quad , \quad 1.42, 6.35, 19.6, 36.26$$

$$Z = 6000 \text{ km} : \beta_{max} = 0.53 \quad , \quad 1.19, 5.84, 18.1, 31.10$$

An important characteristic of  $|\mathbf{E}|_{res}$  is also its *narrow-angle character* in the vicinity of  $F = F_{max}$  (Figs. 10, 11). At these frequencies about 99% of the flux of the electromagnetic waves is concentrated in very narrow angles namely  $\Delta\beta \leq (10^{-1} - 10^{-2})degrees$ .

To compare the data discussed above of the altitude dependence of  $|\mathbf{E}_0|$  and  $|\mathbf{E}_{res}|$ , the values of  $Max|\mathbf{E}_0|_{max}$  and of  $Max|\mathbf{E}_{res}|_{max}$  were normalized to  $Z = 800 \text{ km}$ , namely the dependencies

$$\delta|\mathbf{E}|_{max} = \frac{(Max|\mathbf{E}|_{max} \cdot F_{max}^3)_Z}{(Max|\mathbf{E}|_{max} \cdot F_{max}^3)_{Z=800 \text{ km}}} \quad (23)$$

were calculated. They are shown on Fig.14 and given in Table V, where the altitude dependence of these fields and the values of  $F = F_{max}$  at different altitudes of the Axis field and Resonance field are also given.

Table V. Normalized data of  $|\mathbf{E}_0|$  and  $|\mathbf{E}_{res}|$ .

Z , km	$\delta \mathbf{E}_0 _{\max}$	$ \mathbf{F}_0 _{\max}$ , kHz	$\delta \mathbf{E}_{res} _{\max}$	$ \mathbf{F}_{res} _{\max}$ , kHz	$\frac{Max \mathbf{E}_0 _{\max}}{Max \mathbf{E}_{res} _{\max}}$
800	1	20.60	1	29.6	32
1000	111.34	20.71	43	25.85	71
1500	902.32	16.59	-	-	-
2000	$3.18 \cdot 10^3$	13.02	-	-	-
2500	$8.32 \cdot 10^3$	10.33	-	-	-
3000	$7.29 \cdot 10^3$	8.95	$1.3 \cdot 10^4$	9.55	9.6
4000	$4.51 \cdot 10^3$	6.82	-	-	-
6000	$1.49 \cdot 10^3$	4.26	$3.03 \cdot 10^3$	4.58	81

These data show that the altitude dependencies of the relative maximum values of the Axis and Resonance fields are in general similar. The values of  $|\mathbf{E}|$  increase very quickly by a factor  $\sim 10^4$  in the altitude region  $Z = 800$  to 2400 km, and diminish slow at higher altitudes. The frequencies of  $F_{max}$  are also comparable, but  $F_{0,max}$  is a little smaller than  $F_{res,max}$ . The direction of the maximum values of  $|\mathbf{E}|$ , namely the angles  $\beta_{max}$ , given above in the Tables III and IV, are also commensurable.

The dependence of the  $|\mathbf{E}|$  on the collision frequency  $\nu_{ei}$  at  $z = 1000$  km is shown on Fig. 15 and 16. For both the fields  $|\mathbf{E}_0|$  and  $|\mathbf{E}_{res}|$  the values  $\frac{\nu}{F_{max}} \simeq (1.93 \text{ and } 1.54) 10^{-3}$  when  $\nu_{ei} = 40 \text{ s}^{-1}$ . The maximum values of  $|\mathbf{E}|$  diminish with  $\nu_{ei}$  about 10 times when  $\frac{\nu_{ei}}{F_{max}} \simeq (4.8 \text{ and } 3.0) 10^{-3}$ , namely when  $\nu_{ei} \sim 100 \text{ s}^{-1}$ . Thus, the enhancement of the Axis and Resonance fields is very sensitive to the ion-electron collision frequency which dominates in the altitude region interested us here.

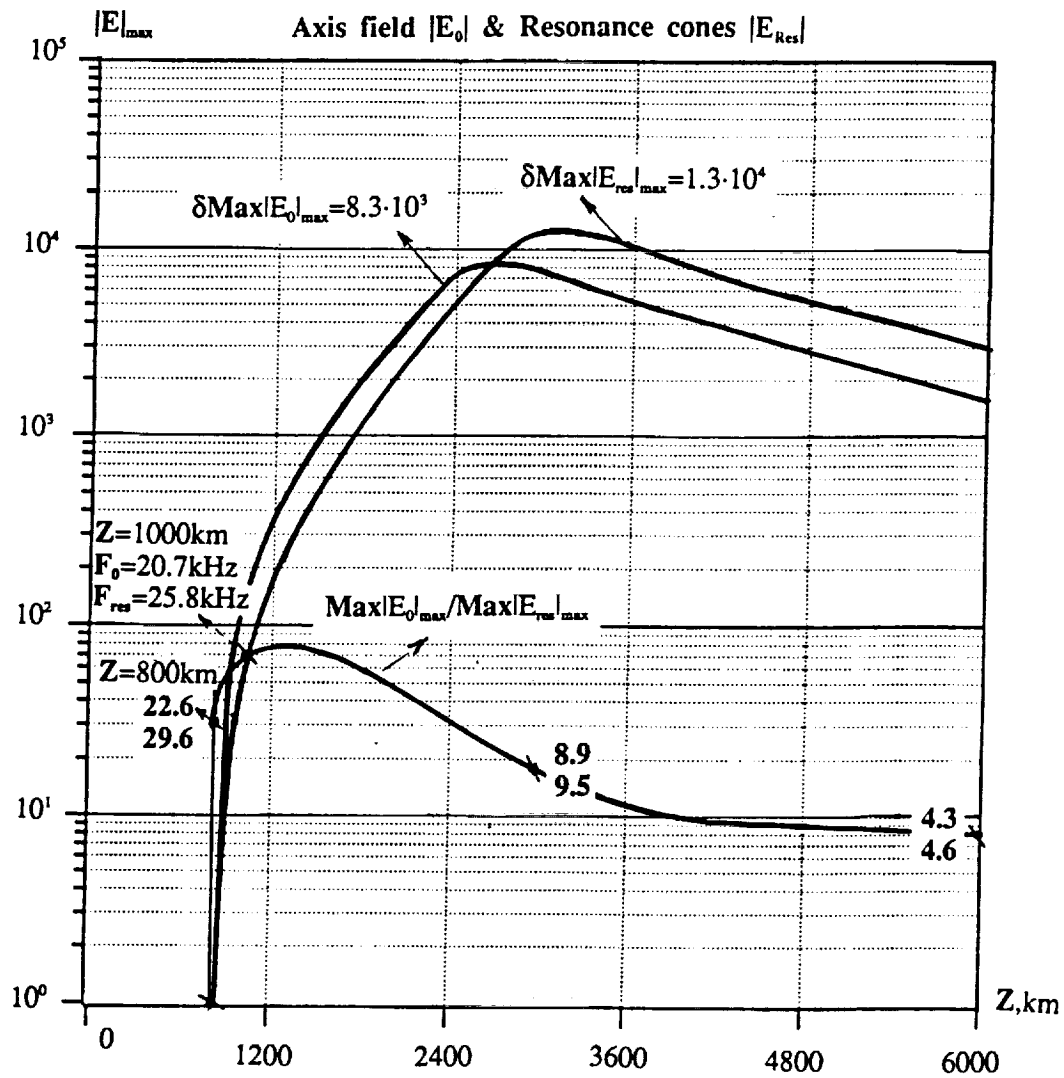
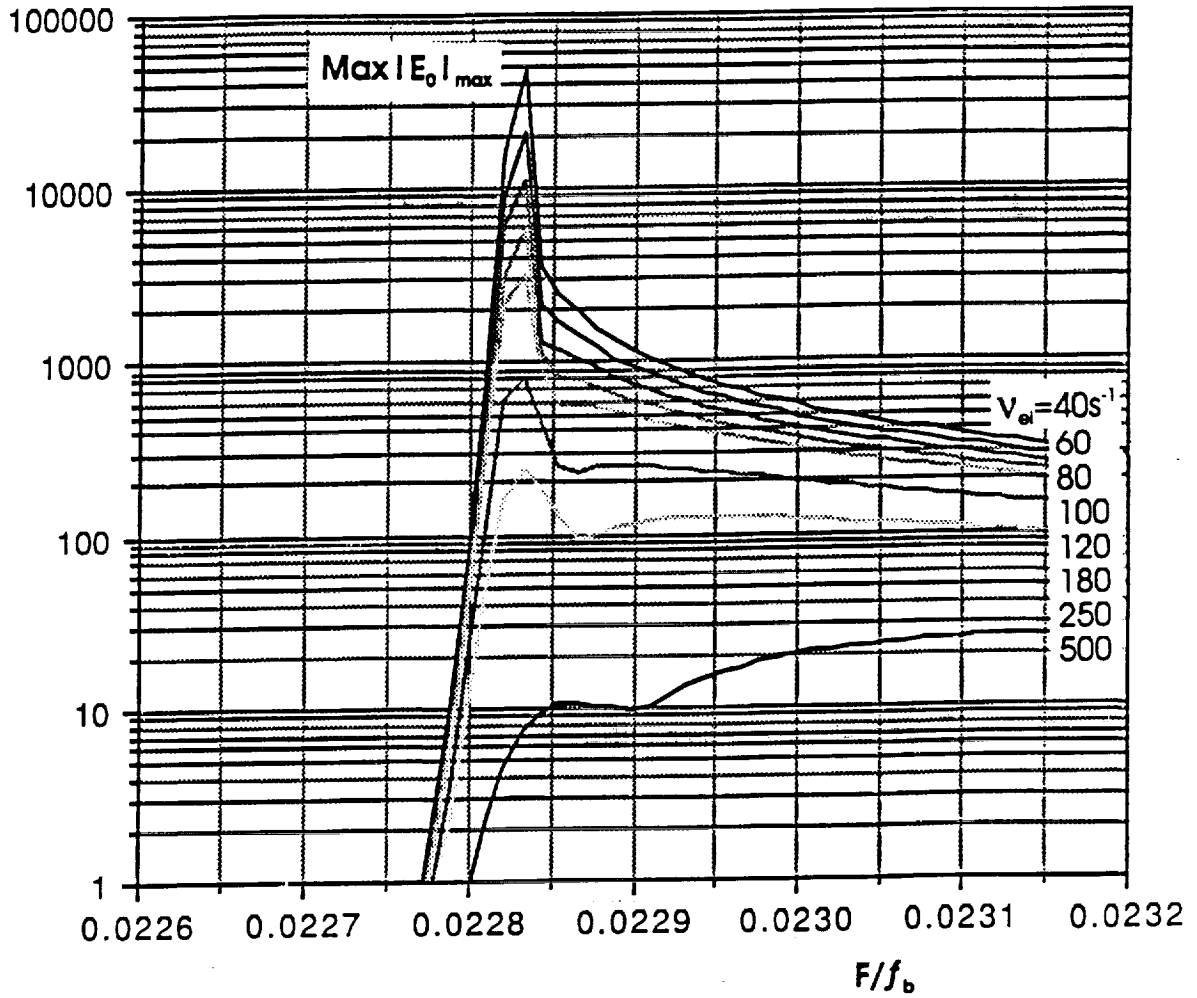


Fig 14. Altitude dependencies of the normalized values of  $|E_0|$  and  $|E_{res}|$ .

### Axis field

$|E_0|_{\max}$   $F_{\max} = 20.71 \cdot 10^3$  Hz,  $f_b = 9.07 \cdot 10^5$  Hz,  $Z = 1000$  km,  $r = 100$  km



**Fig 15.** Frequency dependencies of  $|E_0|$  for different collision frequencies  $\nu_{ei}$ .

**Resonance Cone**  
 $|E_{res}|_{max}$ ,  $Z = 1000$  km,  $r = 100$  km,  $f_b = 9.07 \cdot 10^5$  Hz,  $F/f_b = 0.0285$

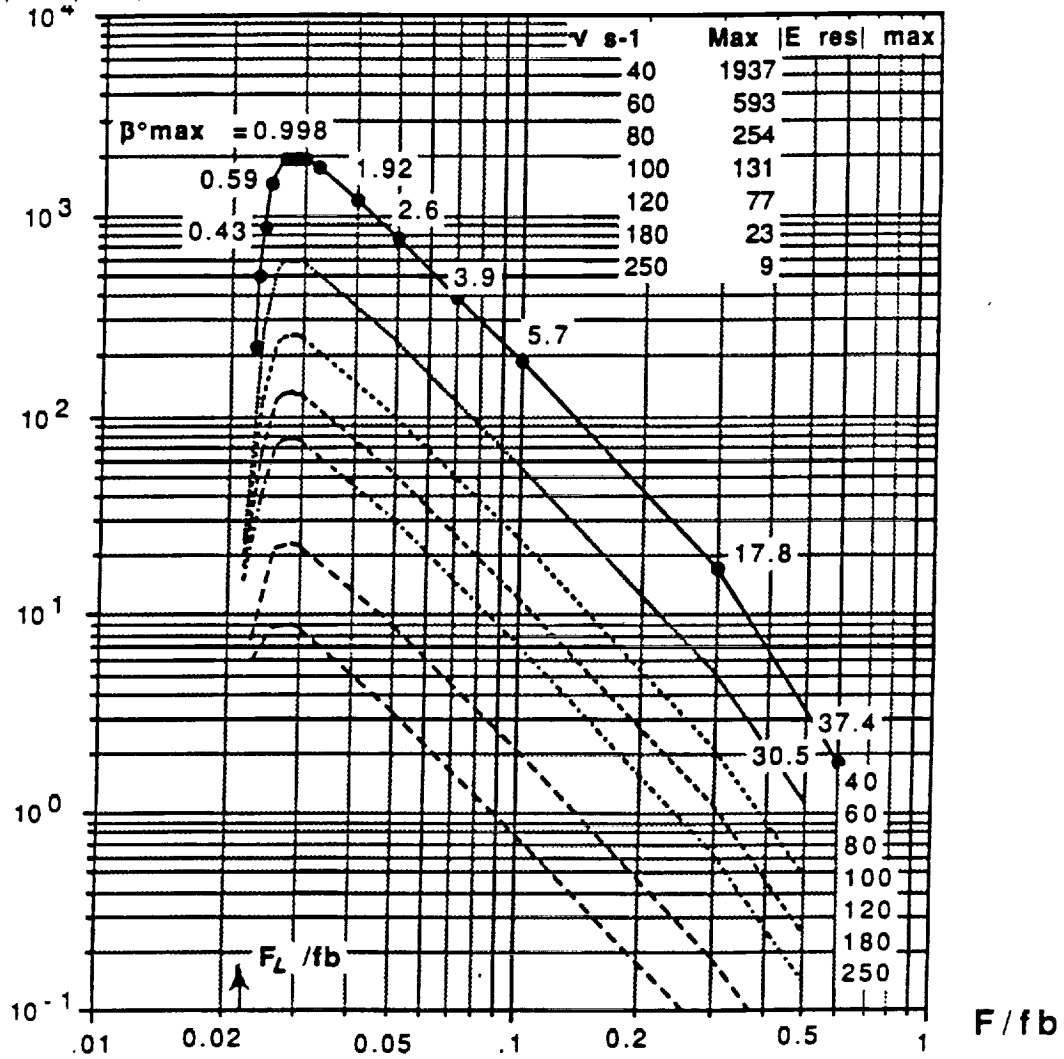


**Fig 16.** Frequency dependencies of  $|E_{res}|$  for different collision frequencies.

## Summary

The results of theoretical investigations of the electric field generated by an electric dipole at different altitudes of the ionosphere and in the low part of the magnetosphere up to  $Z \sim 6000 \text{ km}$  and in the VLF and LF frequency band  $F_b \ll F < f_b$ , where  $f_b$  and  $F_b$  are the electron and ion gyro-frequencies, are given. It is supposed that the source of this field is placed on a satellite which crosses this altitude region of the magnetoplasma and the electric field is recorded on another Sub-satellite moving around the source at distances of (10-s to  $\sim 100 \text{ km}$ ) or a little more. The linear theory for a homogeneous medium may be used by examination of experimental data. The altitude frequency and angle dependencies of the field are studied in the regions of their largest enhancement, these are the Axis field in the vicinity of the direction of the Earth's magnetic field in the two Storey and Resonance cones. One of the most interesting and important peculiarity of this problem is the concentration, focusing of field by a factor of ( $10^2$  to  $10^5$ ) and more in these cones by approaching the low hybrid frequency in the VLF and LF frequency band. The flux of the electromagnetic waves produce in the magnetoplasma due to the caustic focusing, very *narrow pencil beams*. The apexes of these cones are about and even much less than (0.1 to 1) degrees. The principal features of electrical field of these waves are presented above in Sections II.1,2 and III.2.

It is very important and interesting to investigate in detail these predicted theoretical results in situ by experiments on satellites. Such experimental

data will help both, to understand more the physics of different processes in the magnetosphere and also to improve the existing theories of these phenomena. Further theoretical investigation should be done for the study of the guiding of these waves along the magnetic field lines  $\bar{B}_0$  with apogees up to (5 - 6) Earth radii. This theory should be also developed for an inhomogeneous magnetoplasma.

### References

1. Alpert Ya.L., 1989. Proposal P2159-8-89 for NASA, Smithsonian Institution, Astrophysical Observatory.
2. Alpert Ya.L., 1980a, Journ. Atm. Terr. Phys., **42**, 205.
3. Alpert Ya.L. & Moiseyev B.S., 1980b, Journ. Atm. Terr. Phys. **42**, 521.
4. Alpert Ya.L., Budden K.G., Moiseyev B.S. & Stott C.F., 1983, Phil.Trans. Roy. Soc., London **A 309**, 503.
5. Alpert Ya.L., 1983, Ann. of NY Acad. Sci. **401**, 1.
6. Arbel E. & Felsen F.B., 1963, Electromagnetic Theory and Antennas, Part I, 421, edited by B.C. Jordon (Oxford, Pergamon Press).
7. Alpert Ya.L., 1948, Izv. Akad. Nauk, Ser. Fis., **12**, 241, (in Russian).  
See also 1946, Doklady Akad. Nauk, **53**, 703.